

Discussion and extension Annexes C “Fracture Mechanics”

Introduction

This publication is part of compilation of work of the author to a total rigorous theory, containing the latest developments with goal of a thesis and book. The appended articles are mostly given in full as acknowledgment for the original journal publication.

The developed exact theory is given in the appended publications denoted by “C”, thus: vdPut C(1990), C(2000), C(2007a,b), C(2011a,b), C(2012), C(2013), and C(2014). Other important derivations and applications are mentioned in these publications. The new theory in the appended publications and in this discussion is derived by T.A.C.M. van der Put, denoted by: vdPut in the Reference.

Discussion of annexes C about Fracture Mechanics of wood

1. Aspects of new theory, capita selecta

The fracture determining initial cracks in wood are in the principal direction of elastic symmetry of the orthotropic material. When also the direction of crack propagation is collinear with these original cracks, then the fracture criteria of Griffith, Irwin, and Barenblatt are congruent and they can be applied directly to orthotropic plates. Thus at these conditions, the anisotropic fracture problem could be treated by the theory of fracture mechanics for isotropic materials. Because limit analysis applies, virtual displacements apply and solutions are independent of internal equilibrium systems, thus of initial stresses and previous loading histories. The high value of the fracture energy and energy release rate, with respect to the surface energy, shows that a high amount of plastic like dissipation is involved in fracture. Also the blunting at the top of the loading curve of test specimens, visible when the testing rig is stiff enough to allow the test to follow the theoretical softening curve, (the Griffith locus see C(2011a)), shows that there is a plastic range, which is extended enough to make any stress redistribution possible. This confirms that limit analysis has to be applied for the ultimate strength analysis to obtain always possible exact solutions. Limit analysis is based on an elastic-full plastic schematization of the loading curve (see Discussion of annexes D, section D1 for the theory). This means that in stress space, the flow criterion is a single curve and for “plastic” dissipation, the stress vector should be along (tangential to) the concave curve, and the strain vector should be perpendicular to the stress vector (normality rule) what means that the extremum (maximum) variational principle applies for “flow” and thus the virtual work equations apply and thus the theorems of limit analysis with the lower and upper bound solutions existing for any allowable equilibrium system, following as solution of the Airy-Stress function. Fracture of wood thus is a common boundary value problem of the strength at the crack boundary (or boundary of the fractured, plastic zone). This is derived in C(2011a), Chapter 2, and it appears that, for any load combination, fracture occurs by reaching the uniaxial tensile strength at the flat elliptical crack boundary near the crack tip. This uniaxial tensile stress is a measure of the cohesion strength and leads to the mixed mode Wu-equation, eq.(3), as exact solution, as well of the isotropic Airy stress function of the matrix stresses, as for the orthotropic Airy stress function of the total stresses. Only for mode I, is crack extension collinear. For shear, mode II loading, and for combined mode I and II loading, oblique crack extension is determining providing the lower bound solution. Also skipping across fibers (see Fig. 4) is a form of oblique crack extension. Contrarily to this, are all applied methods based on collinear crack propagation of the mathematical flat crack, thus based on the “singularity” approach, which is not able to represent the real, empirical verified, solution for mixed I-II mode fracture (see C(2014) for a

proof). The general accepted singularity approach does not say anything about the local fracture mechanism and the singularity, with infinite fracture stress, does not exist. The center of a crack tip singularity, is an open space. For predicting strength and reliability and for a physical meaning, it is necessary to leave the non-existent singularity approach, which prevents a real description of the ultimate state. Removing a singularity always leads to new theory (see e.g. vdPut B(2011): A new theory of nucleation). Removing the singularity concept for black holes in Astronomy, provided many important new theories where thousands of scientist are working on. Leaving the singularity approach in fracture mechanics, provides the description of real behavior (see C(2007a), C(2011a) C(2011b), with the exact derivation of the mixed I-II mode Wu-equation C(2011a). This last derivation shows a much lower strength by oblique crack extension than at (displaced) collinear extension. The derived Wu-equation, applying for flat elliptic cracks, is:

$$1 = \frac{\sigma_y}{\xi_0 \sigma_t / 2} + \frac{\tau_{xy}^2}{\xi_0^2 \sigma_t^2} \quad (1)$$

Transformation from elliptic to polar coordinates by $\xi_0 = \sqrt{2r_0 / c} \cdot \cos(\delta)$ gives:

$$1 = \frac{\sigma_y \sqrt{\pi c}}{\sigma_t \sqrt{\pi r_0 / 2} \cdot \cos(\delta)} + \frac{(\tau_{xy} \sqrt{\pi c})^2}{(\sigma_t \sqrt{2\pi r_0} \cdot \cos(\delta))^2} = \frac{K_I}{K_{Ic} \cos(\delta)} + \frac{K_{II}^2}{(K_{IIc} \cos(\delta))^2} \quad (2)$$

For collinear crack extension, $\delta \approx 0$, eq.(2) becomes the so called Wu-equation:.

$$1 = \frac{K_I}{K_{Ic}} + \frac{K_{II}^2}{K_{IIc}^2} \quad (3)$$

Eq.(2) shows that for combined (mixed mode) fracture, when $\delta \neq 0$, the apparent stress intensity factors of Irwin, $K_{Ic} \cos(\delta)$, $K_{IIc} \cos(\delta)$ are not constant, and thus are not material constants. The value of δ depends on the loading according to eq.(4), for the isotropic matrix stresses:

$$tg(\delta) = \frac{\sigma_y}{\tau_{xy}} \pm \sqrt{\frac{\sigma_y^2}{\tau_{xy}^2} + 1} \quad (4)$$

For pure mode I: $\delta = 0$, $\tau_{xy} = 0$, is K_{Ic} equal to the Irwin value. For pure shear of the isotropic matrix is $\sigma_y = 0$ and $\delta = 45^\circ$ and is the stress intensity lower than the Irwin value, thus: $K_{IIc} \cos(\pi / 4) = K_{IIc} / \sqrt{2} = 0.71 \cdot K_{IIc}$. This is e.g. measured (in: Eng. Frac. Mech. 78, 16 (2011), Pages 2775-2788) according to Fig.1, for a relatively small initial crack length, in Agathis lumber, (density $480 \pm 10 \text{ kg/m}^3$; 12% m.c. 20 °C). The lumber had no defects, as

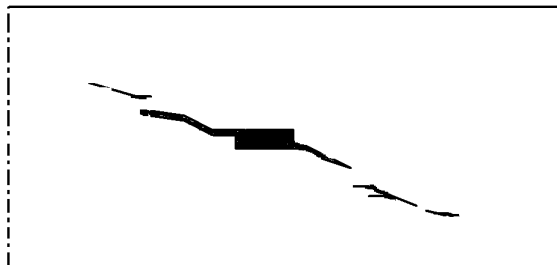


Fig. 1. (see C(2011)) Fracture by pure shear loading by oblique crack extension at the uniaxial ultimate tensile stress (opening mode) near the crack tip in the asymmetric four point bending test with small center-slit. (Sketch after photo of test Eng. Fract. Mech. 2011; 78 - 16: 2775-2788).

knots or grain distortions so that the specimens cut from it were small and clear". Thus, according to the exact lower bound solution of limit analysis, is all fracture a matter of oblique crack extension by failure of the maximal uniaxial tensile stress (cohesion strength) at the crack tip boundary. The oblique angle by eq.(4) is indicated in Fig. 2. This oblique crack extension criterion has to be applied for clear wood as lower bound criterion.

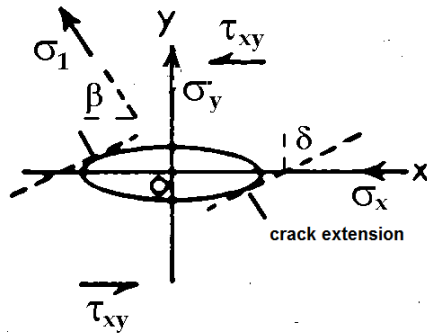


Fig.2. Uniaxial tensile failure at any mixed I-II mode fracture.

Real collinear shear crack extension does not exist, because the tensile stress is zero and there only is a shear stress and only high plastic shear sliding failure would be possible. However, a small crack extension mechanism is possible in the high stressed region near the crack tip and a displaced collinear crack extension is possible by tensile failure as indicated by fig. 3, where after oblique crack extension, small crack extension from the fractured zone to the macro crack tip occurs, or a jump over fibres, as given by Fig. 4, is possible for wood, where separate small cracks extend by tensile failure. This has the same effect as macro-crack extension at a small value of δ , and thus $\cos(\delta) \approx 1$, and eq.(3) applies nearly precisely for timber. This is not only verified by the data of Wu, but also e.g. by the mixed mode fracture mechanics tests of Murphy et al, done at the TL-system on eastern red spruce at normal climate conditions using different kinds of test specimens. The usual finite element calculations provided the geometric correction factors, and the stress intensity factors and a lack of fit test was performed on the data, at the for wood usual variability, assuming five different failure equations. Statistical lack of fit values are tabulated in Table 1 below and as can be seen from that table, the one failure criterion, that cannot be rejected due to lack of fit, is the by Wu- equation, eq.(3), which also is shown to fit wood with small defects as failure criterion and is derived exactly in C(2011a) and is equal to the real solution.

Table 1. Lack of fit values for arbitrary failure criteria

Failure criterion	p value
$K_I / K_{Ic} = 1$	0.0001
$K_I / K_{Ic} + K_{II} / K_{IIc} = 1$	0.0001
$K_I / K_{Ic} + (K_{II} / K_{IIc})^2 = 1$	0.5629
$(K_I / K_{Ic})^2 + K_{II} / K_{IIc} = 1$	0.0784
$(K_I / K_{Ic})^2 + (K_{II} / K_{IIc})^2 = 1$	0.0001

As directly appears from the mode II test, is the pure sliding mode of Irwin not existent, and is tensile failure, with opening mode, always the cause of any crack extension. In C(2012), §4, and below at Fig. 10, this is shown to apply for the standard mode II bending test. For small crack extension is collinear crack extension possible by interference of tensile

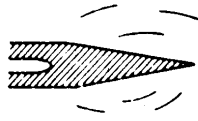


Fig. 3 Craze at the crack tip and possible crack extension along the fractured zone in glassy polymers.



Fig. 4 Scheme of Wu, of crack extension by skipping across fibers

stresses, causing tensile failure in the weakest plane (along the grain) as is given by Fig. 5, by small crack merging, where each small crack is propagating in the two directions towards the neighboring cracks. This is the principle of the small crack merging mechanism of C(2011a).

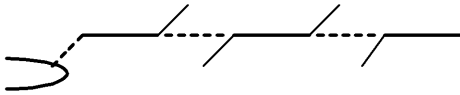


Fig. 5. Collinear small crack merging.

In C(2014), the exact derivation of the geometric correction factor of the center notched test specimen is given, based on small cracks merging as explanation of softening behavior. The failure criterion of clear wood and of timber (A(2009), A(1982a), and the failure criterion by a single macro notch (C(2011a), C(2014)), are the same, showing that small-crack extension towards the macro-crack tip is the cause of macro-crack extension. This is confirmed by the fact that the stress intensity factor is the same independent on the macro-form and dimensions of the notch. It also is confirmed by molecular deformation kinetics, showing the same processes in clear- and in notched wood (see discussion Annexes B). Also the exact solutions given in C(2014) of the geometric correction factor and of C(2012) of the strength behavior of long post-critical crack lengths is totally based on small crack behavior. The small-crack merging mechanism explains, in C(2011a), precisely the mode I softening curves of Boström (1992). The failure criterion A(2009) shows no coupling term between the normal stresses at “flow”, and thus shows no dowel action of the reinforcements and there only is a direct interaction of the reinforcement with the matrix and the matrix stresses determine the stresses in the reinforcements. Because the initial small cracks in wood are in the matrix and start to extend in the matrix, the stress equilibrium condition of the matrix by the matrix-stresses has to be regarded. The isotropic solution of the matrix stresses thus has to be regarded in the end state. The total stresses, due to the reinforcement, then follow by multiplication of an elastic constants factor (e.g. derived in Section 2 of C(2011a)).

Contrarily to what is stated by Fig. 6, is all fracture mechanics nonlinear. However, the linear approach (LEFM) is always applicable and is exact in the form of limit analysis which is based on the linear-full plastic schematization of the loading curve. The full-plastic zone is given by a single curve in stress space as shown in Fig. 6. In Fig. 6 is d/d_0 , the ratio of specimen size to the fracture process zone size. But, because the volume effect is tested, is the initial crack length proportional to the specimen length. Thus, d/d_0 also can be regarded to be the ratio initial open crack length to the process zone size. Then, for small values of d ,

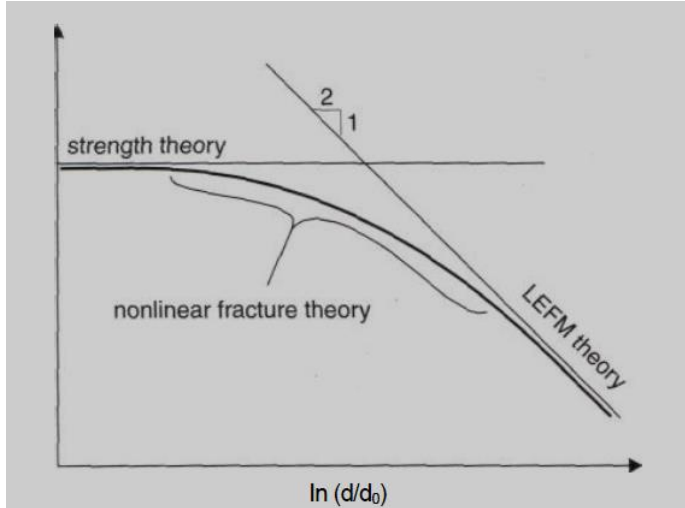


Fig. 6. from: “Fracture and Fatigue in Wood” of I.Smith et al showing wrong interpretations.

this d/d_0 ratio also may represent the critical small crack density in a macro specimen (d also is crack interspace). The curved line of fig. 6, follows the equation:

$$\ln \sigma = \ln \sigma_0 - 0.5 \ln(1 + d/d_0)$$

This can be written:

$$\ln\left(\frac{\sigma}{\sigma_0}\right) = \ln\left(\frac{d_0 + d}{d_0}\right)^{-0.5} = \ln\left(\frac{d_0}{d_0 + d}\right)^{0.5}$$

$$\text{or: } \sigma \sqrt{d_0 + d} = \sigma_0 \sqrt{d_0} = K_c / \sqrt{\pi},$$

showing the curve to represent the stress intensity as ultimate state with K_c as critical stress intensity factor.

It further is shown that for values of $d/d_0 \gg 1$, the curved line approaches the drawn straight tangent line

and thus is then the slope of the curve

$\ln \sigma = \ln \sigma_0 - 0.5 \cdot \ln(1 + d/d_0) \approx \ln \sigma_0 - 0.5 \ln(d/d_0)$ as limit. The real slope however is:

$$\frac{\partial \ln \sigma}{\partial \ln(d/d_0)} = \frac{\partial \ln \sigma}{(d_0/d) \partial(d/d_0)} = -\frac{d}{d_0} \cdot \frac{0.5}{1 + d/d_0} = \frac{-0.5}{1 + d_0/d}$$

This slope is: -0.5 for $d \gg d_0$ and this slope is zero when $d = 0$.

This shows that for the whole curve LEFM (linear elastic fracture mechanics) applies and it is an indication that, at zero dimensions, thus zero $d = 0$, the strength theory still follows LEFM, because it applies also for initial length d_0 . The strength theory applies for ultimate high loaded areas according the small crack merging mechanism, when the critical small crack density is reached. This means that the small crack spacing is about the small crack length (see C(2011a), section 3.6) and this applies for any initial small crack length $d + d_0$.

However, when d_0 is of the order of d , the crack length and thus the crack spacing, there only is plastic flow in the intact ligament material. For wood this is determining for very small specimens, or for small loaded areas. For instance, the maximal bending tension stress occurs at one point and thus maximal bending tension occurs at a small area and will be plastic. For wood loaded in bending and compression therefor is the ratio bending tension to bending compression $s = f_{m,t} / f_c$ constant (and thus both plastic), as shown in D(2012b), for any load combination of bending with compression, indicating also that there always is failure by the ultimate bending tensile strength. A volume effect by stress distribution thus needs not to be regarded. The volume effect thus now is caused by the volume alone due to decreasing quality by volume increase (For that reason also the compression strength may show a volume effect).

Because, as mentioned before, the isotropic matrix “flows”, before the reinforcement, limit analysis has to be applied for the isotropic stresses in the isotropic matrix. This is not followed by all other methods, which therefore don’t satisfy the failure criterion and are not able to give the right exact mixed mode fracture criterion. At initial flow of the matrix, the

stresses of the still elastic reinforcement follow in proportion the matrix stresses. That the matrix is first determining follows e.g. for Balsa wood, which is highly orthotropic, but is light, thus has a low reinforcement content and shows total failure soon after matrix failure and thus shows at failure the isotropic ratio of $K_{IIc} / K_{Ic} \approx 2$ of the isotropic matrix material. But also for strong clear wood which is failing by shear by single oblique crack extension according to Fig. 3, it appears that the start of crack extension shows the isotropic oblique angle, showing the matrix to be determining for initial failure. The truss action, at bending failure of a beam, causes a negative contraction coefficient in the bending tension zone. This shows that the reinforcement holds, even after flow in compression and stress redistribution, with increased tension in the reinforcement. It is therefore a requirement for an exact orthotropic solution of the total applied stress, applicable to wood, to also satisfy the isotropic flow solution of the matrix-stresses.

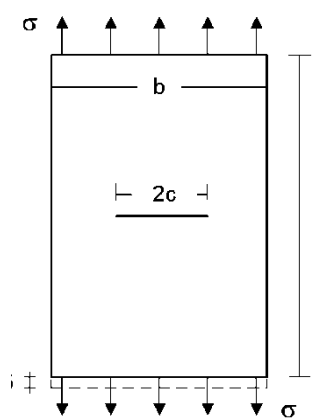
As discussed at Annexes A, the (small crack) failure criterion for shear with tension is:

$$F_2\sigma_2 + F_{22}\sigma_2^2 + F_{66}\sigma_6^2 + 3F_{266}\sigma_2\sigma_6^2 = 1 \quad (5)$$

$$\text{Thus: } \frac{\sigma_6}{S} = \sqrt{\frac{(1 - \sigma_2/Y) \cdot (1 + \sigma_2/Y')}{1 + c\sigma_2/Y'}} \approx \sqrt{1 - \sigma_2/Y} \quad (6)$$

This becomes, as limit behavior, equal to the Wu-equation when due to full hardening $c \rightarrow 1$. Full hardening is possible when the test rig is stiff enough to remain stable during test. The solution of the crack problem of Irwin as summation of in plane and antiplane solutions in order to use, (with minor adaptations) isotropic stress functions for the orthotropic case, and to apply descriptions in the three characteristic modes and to sum the result for the general mixed mode case is not right for wood, because the failure equation is not orthotropic, eq.(5) is not quadratic but contains a third order term and thus is not orthotropic symmetric. This coupling term is absent in the general accepted Sih-, Paris-, Irwin solution. The stress function which leads directly to the Wu-equation is known and given in C(2011a), § 2.3.

The Griffith strength equation, based on virtual crack extension, eq.(3.8) of C(2011a):



$$\sigma_y^2 = G_c E_y / \pi c \quad (7)$$

can be extended by superposition to:

$$\sigma_y^2 + \tau_{xy}^2 = G_c E_y / \pi c \quad (8)$$

This exact law, only can be right, when G_c is not a material constant but is a function of σ_y and τ_{xy} , because G_c varies between G_{Ic} and G_{IIc}

In orthotropic stresses, is eq.(8):

$$\sigma_y^2 + \tau_{xy}^2 / n_6^2 = G_f E_y / \pi c \quad (\text{see C(2011a)})$$

Fig.7.Center notched mode I specimen

The reason that G_c in eq.(8) is variable follows from the global stresses (stresses ad infinitum), which are not based on the local stresses at the crack tip. Therefore G_c in eq.(8) can be G_{Ic} , because also elastic shear stress can be dissipated at a mode I fracture. Necessary thus are the stresses at the crack boundary to know the mode of failure. This follows from the exact derivation in C(2011a) and is applied by the virtual crack closure technique of finite element simulation, but is based on a separate calculation of the energy release rates of the normal stress in the opening mode and of the shear stress in the sliding mode following the method of Sih, Paris, Irwin by giving the sum of separate solutions for the 3 modes, without interactions, what is assumed to be possible by assumed isotropic and orthotropic symmetry. This however is against eq.(5) because the

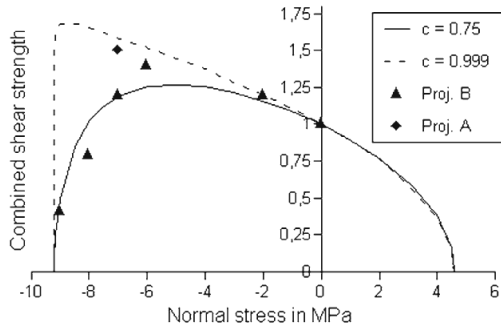


Fig. 8. Eq.(5), influence of $3F_{266}\sigma_2\sigma_6^2$, with the dashed parabolic limit line of eq.(6)

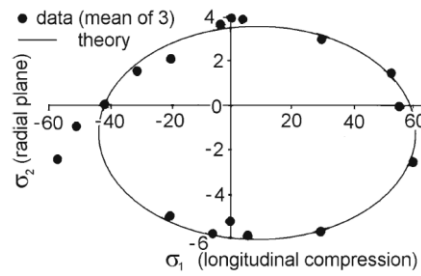


Fig. 9: Also same hardening at compression to parabolic data outside the elliptic curve (due to slip line formation).

coupling between work by normal and by shear stresses, as given by $3F_{266}\sigma_2\sigma_6^2$ in eq.(5), is not present in the existing methods and “mixed mode” interactions as given by Fig. 8 and 9 can not be described by other methods as e.g. of Sih, Paris and Irwin.

Figure 10 explains why, in the mode II standard test, under shear loading, not a sliding mode II, but an opening mode I tensile failure occurs.

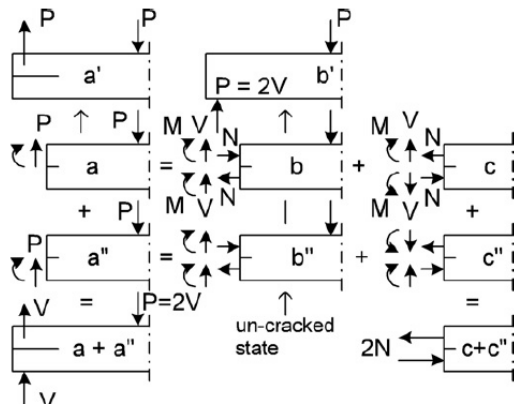


Fig. 10. Fracture loading of the single end notch beam

In Fig. 10, the “mode II” test is represented by case $a + a''$. If the sign of the lower reaction force V of this case is reversed and $P = 0$, the loading of the mode I, double cantilever beam (DCB) test is obtained, identical to loading case c with $N = 0$. In Fig. 10, case $a + a''$ is split in case a and in case a'' , as loading of the upper and the lower cantilever. Case a is identical to case a' which is similar to end-notched beams discussed in C(2011a), Chapter 6. This case behaves like the mode I fracture test as can be seen by loading case c . The loading near the crack tip, given by case a , can be seen as the result of superposition of the stresses of cases b and c , where the loading of case b is such, that the un-cracked state of the beam, case b' , occurs. The loading of case c is such that the sum of cases b and c gives loading case a . Case c is the real crack problem and the critical value of strain energy release rate G_c can be found by calculating the differences of elastic strain energies between case a' and b' , the cracked and un-cracked system C(2011a). Case c shows the loading of the mode I – DCB-test by V and M , combined with shear loading by N and the energy release rate thus will be somewhat smaller (by this combination with N) than the value of the pure DCB-test. For the loading case a'' , the same stresses occur as in case a , however with opposite directions of M and V with respect to those of case c , according to case c'' , causing crack

closure. To prevent that crack closure c'' , and friction, dominates above crack opening c , the crack slit has to be filled with a Teflon sheet. By superposition of cases c and c'' , case $c + c''$ of shear loading of pure mode II occurs, as crack problem due to the total loading. The normal load couple of $2N$ is just the amount to close the horizontal shift of both beam ends with respect to each other at that loading stage. This explains the applicability of the virtual crack closure technique.

Because the upper cantilever is stronger for shear than the lower cantilever, because of higher compression perpendicular and along the grain (see Fig. 8), mechanism c will dominate above c'' , when the lower cantilever start to flow in shear. Thus mode I, case c tensile failure occurs.

2. Softening behavior and correction of the fracture energy C(2007a)

When crack extension occurs in a cantilever beam loaded by a constant load P at the free end, then the load gets a deflection δ due to this crack extension, then the work done on the beam is $P \cdot \delta$ and the work for the elastic strain increase is: $P \cdot \delta / 2$. Then the work for crack extension is $P \cdot \delta - P \cdot \delta / 2 = P \cdot \delta / 2$, thus equal to the elastic work of strain increase. Therefore is the area under the load-displacement softening curve the total external work on the test specimen and not the fracture energy. The fracture energy follows from half this area what is equal to the critical strain energy release rate at the first crack increment. For wood this correctly is applied for mode II. See Fig. 11 below, where the elastic part of stored energy is subtracted from the total applied energy of the loading curve to get the right fracture energy. For mode I however, as for other materials, wrongly the total area is regarded as fracture energy, thus a factor 2 too high, as shown in C(2007a). Softening of a real stress on intact material does not exist. The softening stress is a nominal stress and thus a measure of the stress outside the fracture plane. In the fracture plane acts the mean ultimate failure stress. The measurements at softening may show an apparent decrease of the specific fracture energy C(2011a) when related to one extending crack. This can be explained by a multi small crack joining mechanism when the critical; small crack density is reached, thus the ultimate state of the remaining intact ligament length of the test-specimen. Post fracture behavior thus is not comparable with the behavior of macro crack initiation. It further is shown, by the kinetics of the process, that the irreversible work of an ultimate loading cycle is proportional to the activation energy of the fracture process and not to the driving force of the process. This explains why the crack velocity decreases with the increase of this

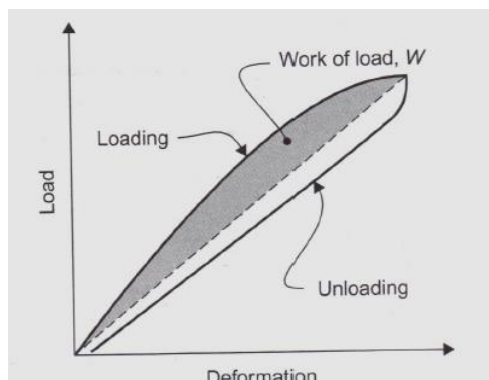


Fig.11.Mode II fracture energy book of I. Smith et al

irreversible work, and increases with the stress intensity increase.

The fracture energy is a function of the Griffith strength and thus is related to the effective width of the test specimen and not to the ligament length. This also has to be corrected. Based on the derivation of the softening curve, the in Boström (1992), reported fracture toughness of 720 kNm, of double-edge notched tests, is corrected to 330 kNm and the value of 467 kNm, based on the fracture energy, of the compact tension tests, also is corrected to the right value of 330 kNm. A revision of published mode I data, based on the fracture energy obtained by the area under the softening curve, thus is necessary.

The concluding final theory is given in C(2007a).

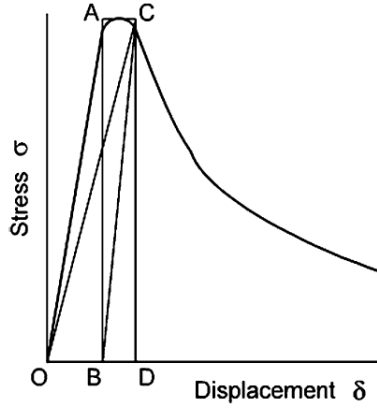


Fig 12. Stress- displacement of specimen Fig. 7

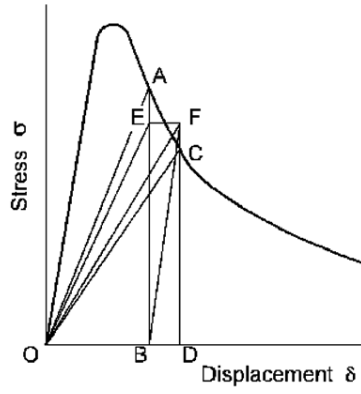


Fig 13. Descending branch of Fig.12.

In the elastic-full plastic schematization of limit design is, in Fig. 12, the area OAB, written here as A_{OAB} , the strain energy of the specimen of Fig. 7, with a central crack (or with two side cracks) with a width “ b ”, length “ l ” and thickness “ t ”, loaded to the stress σ . During the quasi static crack extension from B to D, in Figure 12, the constant external load σ does the work on the specimen of: $\sigma \cdot b \cdot t \cdot \Delta \varepsilon_{BD} \cdot l = \sigma \cdot b \cdot t \cdot \delta_{BD} = A_{ABDC}$, where $\Delta \varepsilon_{BD}$ is the strain increase due to the cracking and δ_{BD} the corresponding displacement. The strain energy after the crack extension is A_{OCD} and the strain energy increase by the crack extension thus is in

Fig. 12: $A_{OCD} - A_{OAB} = A_{OCD} - A_{OCB} = A_{CBD} = A_{ABDC} / 2$. Thus half of the external energy $A_{ABDC} = \sigma \cdot b \cdot t \cdot \delta_{BD} / 2$ is the amount of increase of the strain energy due to the elongation by δ , and the other half thus is the fracture energy which is equal to this increase of strain energy. The same follows at unloading at yield drop. Because every point of the softening curve gives the Griffith strength, which decreases with increasing crack length, unloading is necessary to maintain equilibrium. The fracture with unloading step AC in Fig. 13 is energetic equivalent to the unloading steps AE and FC and the fracturing step EF at constant stress $EB = FD = (AB + DC)/2$. Thus $A_{ABDC} = A_{EBDF}$, Identical to the first case of Fig. 12, the increase in strain energy due to crack extension is:

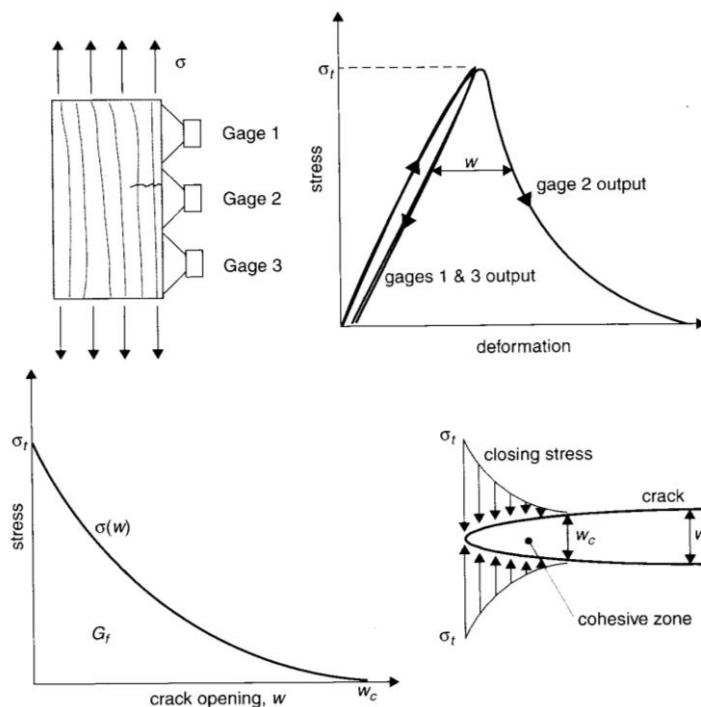
$A_{ODF} - A_{OBE} = A_{ODF} - A_{OBF} = A_{BFD} = 0.5 \cdot A_{EBDF} = 0.5 \cdot A_{ABDC}$, equal to half the work done by the external stresses during crack propagation and thus also equal to the other half, the work of crack extension. It thus is shown that half the area under the load-displacement curve represents the fracture energy. For mode II, only line OACO in Fig. 12 is measured and A_{OAC} is regarded to be the fracture energy (see Fig. 11). Because $A_{OAC} = A_{BAC} = 0.5 \cdot A_{ABDC}$, thus equal to half the area under the load displacement curve, the right value is measured and mode II data need no correction.

3. Weibull size effect in fracture mechanics of wide angle notched beams

A new explanation is given in chapter 9 of C(2011a) of the strength of wide angled notched timber beams by accounting for a Weibull type size effect in fracture mechanics. The strength of wood is described by the probability of critical initial small crack lengths. This effect is opposed by toughening by the probability of having a less critical crack tip curvature. The toughening effect dominates at the different wide angle notched beams showing different high stressed areas and thus different influences of the volume effect. The explanation by the Weibull effect implicates the determining small crack extension,

4. Discussion of Cohesive zone models

Nearly all assumptions of the cohesive zone models are against theory. The most fundamental violence is to regard the stress of the softening curve, which is a nominal stress,



Fictitious crack model development.

Fig. 14. of Fracture mechanics book of I. Smith et al

thus, a stress far outside the fracture plane, to be the stress in the fracture plane (the ligament), while the real stress shows hardening in stead of softening and thus shows no impossible negative dissipation and stiffness. The aim of the cohesive zone model was to remove infinite tensile stresses of the singularity method, by substitution of an internal compressional equilibrium system which neutralizes the singularity. However, this superposition of closing stresses is superfluous because the singularity does not exist and the singularity solution, or mathematical flat crack solution, also is an approximation. The singularity is an empty space within the crack boundaries and there thus is no material which can be stressed infinitely high. The crack problem thus is a common limit analysis boundary value problem at the crack boundary, or better, at the elastic-plastic boundary of the plastic and fractured zone around the crack and crack tip. All kinds of dissipation within this boundary determines the fracture energy (= energy release rate). The exact solution of the Airy stress function is given in e.g. C(2011a), showing that fracture always occurs by reaching the uniaxial ultimate, tensile stress (cohesion strength) near the crack tip, what leads to the parabolic Wu-mixed mode initial failure criterion, eq.(1), which thus is the exact criterion, is in accordance with the measurements of precise tests (of Wu and Murphy). By this solution (of C(2011a)), the real “traction stresses” near the crack tip are known and it is not necessary to assume an arbitrary impossible system with negative dissipation and negative spring constants. In Fig. 14, the assumed internal compressional equilibrium system is given, which follows from the, by gage 2 measured, unloading of the specimen, what wrongly is assumed to represent a crack opening law, (with negative spring constant). The real fracture energy, follows from the total external applied load, and thus the total elastic deformation increase of the whole specimen has to be measured. Measuring deformation over a crack opening has no meaning because it is not known what is measured. The local stress decrease by local unloading is no measure of the increase of stress in the remaining intact ligament. In Fig. 15, the stress and strain at the points A are zero, due to the unloaded triangles adjacent to the crack, and the crack opening will be proportional to the crack length a by unloading, and is not related to the constant mean ultimate stress of the remaining intact ligament. The area under the load – total displacement curve determines the total applied external work on the specimen. Half of this area is the elastic strain increase and the other half is the fracture energy (= equal to the

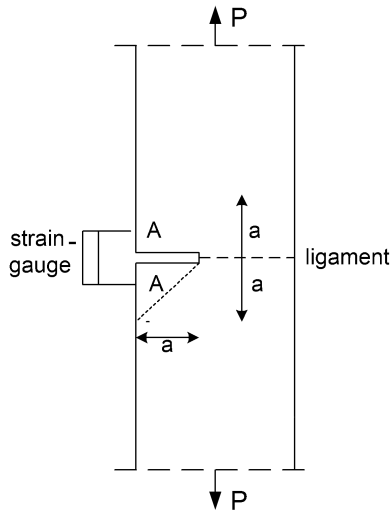


Fig. 15 Nonsense data

elastic energy increase). The cohesive zone model regards the total area, thus the total external energy as fracture energy, thus a factor 2 too high (see Section 2). Further is this energy wrongly related to the area of the crack length increase instead of to the total crack length area, including the initial crack length. By doing so, the fracture energy per unit area (which should be equal to the energy release rate) is not a material constant but depends on the chosen initial crack length. Further, the total measured energy has to be divided among the different acting processes. The activation energy tells which process is the fracture process. The cohesive zone model does not account for this result of the exact theory of molecular deformation kinetics, (see B(1989a)). This theory also explains why softening only is possible in a constant strain rate test and is not possible in a constant loading rate test and in a dead load test to failure.

Because in practice only dead load failure occurs, is it astonishing that impossible softening is regarded as traction law instead of the elastic-plastic diagram of dead load loading. A severe lack of distinction of acting kinetic flow processes is made by the cohesive zone model of dowel connections in wood. Most investigations on connections are with one- or a few dowels, where the dowel is determining for initial “flow”. This applies especially for the in practice applied slender dowels, thus up to connections with 9 to 12 nails. Then the dowel is determining for initial failure and splitting of the beam occurs at flow and hardening of the embedment, because the dowel performs a crack opening movement at embedment failure. Thus the spreading effect of the embedment strength of the dowel, then determines the splitting strength of the joint. The tri-axial compressional hardening effect of the dowel embedment should be accounted in the models. The exact derivation, as boundary value solution, based on the shear-line (called slip-line) construction, of the embedding strength is given in vdPut D(2008b), with the simplification to the simple spreading model. In the 2D cohesive zone model for dowel-connections of Franke (see Fig. 16) is the measured triaxial compressional hardening regarded to be a tensional hardening leading to random results, with an extreme high variability, and a statistical exclusion of fit to any equation. The cohesive

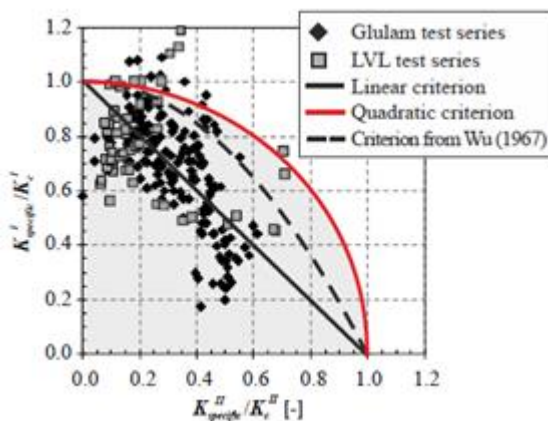


Fig. 16. Failure according to cohesive zone model

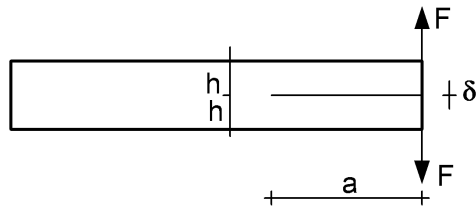
zone model behavior is too far away from real behavior thus according to exact theory. The reason of this mismatch lies in the method itself because nearly all model assumptions made are strongly against exact theory and generally against thermodynamics and even the tensile strength is not ultimate but variable down to zero (called cohesive forces). Strain softening in this case cannot exist and is not measured. The Griffith stress of e.g. the center notched specimen is $\sigma_g = \sqrt{G_c E' / \pi a}$.

This is a nominal stress, thus is occurring in the intact elastic part of the specimen, far outside the fracture plane, (the stress ad infinitum) and is not the real failure stress.

The real mean stress in the fracture plane, the still intact ligament, is a factor $b / (b - 2a)$

higher and is an increasing stress: $\sigma_{gr} = (\sqrt{G_c E / \pi a}) / (1 - 2a/b)$ increasing with the increase of the crack length a (see C(2011a), eq.3.10). It is thus necessary to speak of hardening because the stress in the critical section increases at crack extension (until a maximum value).

The by some cohesive zone models applied “delamination test”, to determine the traction force, should be in accordance with exact theory. The calculation is as follows, according to Fig.17: The deformation δ of the upper plus the lower cantilever parts of the beam of figure 17 is:



$\delta = (8Pa^3) / (Eb^3)$ and thus is the compliance:

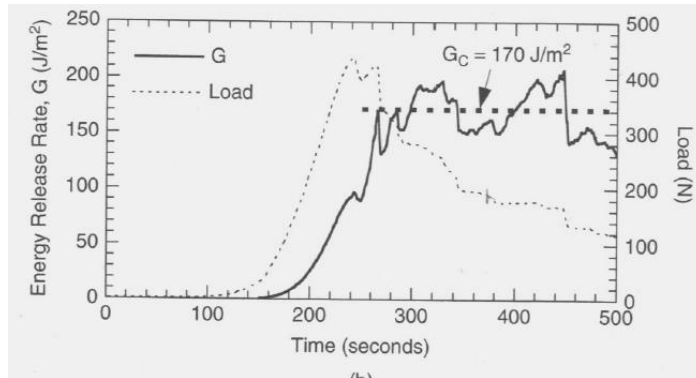
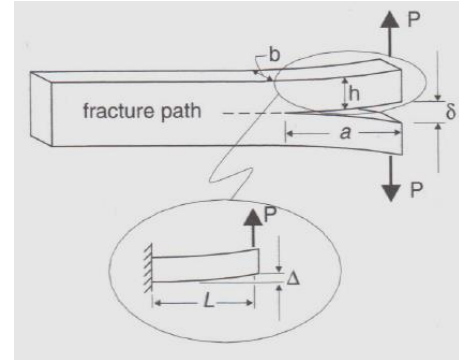
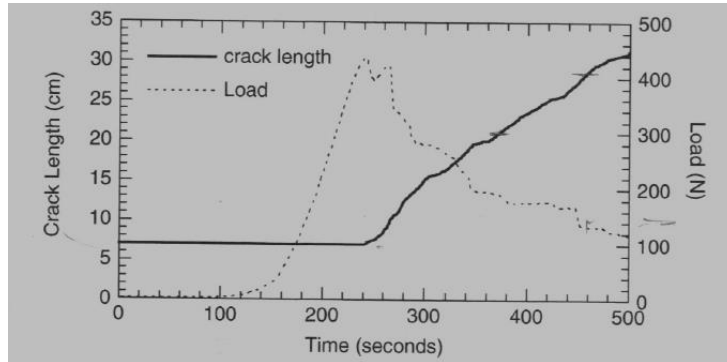
$C = (8a^3) / (Eb^3)$ and the energy release rate:

$G_c = (F^2 / 2b)(dC / da) = (12F^2 a^2) / (Eb^2 h^3)$

and accounting also for the shear deformation as in C(2011a), sections 6 and 7, G_c becomes:

$G_c = (12F^2 / Eb^2 h) [(a^2 / h^2) + (E / 10G)]$ Thus:

Fig. 17. Delamination test



The strain energy release rate G is:

$$G = \frac{1}{2b} P^2 \frac{dC}{da}$$

$$G = \frac{1}{2b} P^2 \frac{dC}{da} = \frac{1}{2b} P^2 \frac{d}{da} \left(\frac{8a^3}{Eb^3} \right) =$$

$$= \frac{12P^2 a^2}{Eb^2 h^3} \quad (9)$$

or when shear deformation is included this becomes:

$$\frac{F}{bh} = \frac{\sqrt{EG_c / h}}{\sqrt{12a^2 / h^2 + 1.2E / G}} \quad (10)$$

Fig. 18. Empirical confirmation of theory

At the start is the term $1.2E / G$ dominating, giving an ultimate shear stress criterion:

$$f_v = \frac{F}{(2/3)bh} = \sqrt{GG_c}$$

For very long cracks is possible:

$$\frac{F}{bh} \approx \frac{\sqrt{EG_c / 12h}}{a/h} \text{ or } f_m = \frac{Fa}{bh^2 / 6} = \sqrt{\frac{3EG_c}{h}}$$

giving the “traction stress” of cohesive zone model, now based on positive stiffness and dissipation. At a constant strain rate test, also the

rate of crack extension is constant. The requirement $F \cdot a = C_1 = \text{constant}$, is needed for a constant bending strength. The external loading F has to diminish at increase of crack-length a , which acts as increase of the lever arm, in order to have a constant traction at the crack tip of the constant cohesive tensile stress, for a constant value of the fracture energy G_c . Thus there is unloading of F and no softening of the strength in the fracture plane, but a constant critical ultimate stress in the critical zone.

At the end stage of crack extension, the remaining future crack plane is high loaded and shows additional damage, by micro-crack extension and merging, to- and outside the macro-crack tip, causing an apparent decrease of G_c (when this is related to one macro-crack extension alone). Again this is not a real decrease of G_c , but a more efficient use of fracture energy (vdPut C(2011a)). Thus; the term “softening “ has to be replaced by “elastic unloading” (applying for this stress at infinitum, outside the fracture plane).

The confirmation of theory by data is not done in the right way by Fig. 18. First the theoretical derivation of the dashed loading curve should be given (as done in C(2011a), section 3.3) and then the curve should be fit to the data (without need of negative dissipation and negative stiffness). Then it is possible to notice the departure from theory by multiple small crack propagation in the end state of the test, when the remaining, still intact, ligament is high loaded (see section 3.6 of C(2011a)).

5. The energy approach of fracture of beams by joints loaded perpendicular to grain

The derivation, based on the compliance method of fracture mechanics, is given in C(2011a) and will be discussed further. The apparent brittle failure of fracture mechanics tests is due to instability by too low stiffness of specimens and testing equipment. The testing of Boström (1992), at sufficient stiffness to follow the theoretical softening curve, shows sufficient plasticity near and at the rounded top for total stress redistribution. This means that limit analysis has to be applied for the ultimate strength analysis providing always possible exact solutions. Because the extremum, (the ultimate value), is not dependent on the followed loading path, the analysis can be based on an elastic-full plastic schematization of the loading curve. This means that the full plastic flow criterion is a single curve in stress space and for “plastic” dissipation, the stress vector should be along (tangential to) the concave curve, and the strain vector should be perpendicular to the stress (normality rule) what means that the (maximum) extremum variational principle applies for “flow” and thus the virtual work equations apply and thus the theorems of limit analysis, with the lower and upper bound solutions, applying for any allowable equilibrium system, (e.g. following as solution of the Airy-Stress function). In these virtual first order calculations of small changes, the strength is, except the independence of the loading path, also not dependent on initial stress and internal equilibrium systems. It therefore is necessary to apply common beam theory, as small, first expanded, behavior, which can be regarded to differ an internal equilibrium system from the real stress state. This also can be stated as follows: Because an internal equilibrium system has no influence on the ultimate strength, the differences of the potential energy of this system, of the cracked, and the un-cracked, intact state, should not be accounted and only the first order term has to be regarded. Also lower order effects, as clamping action and lower order bending terms have to be omitted for the highest lower bound solution. Thus the beam theory has to be applied solely for the right solution (and thus forget the upper bound finite element calculation). This is applied here for the tested beams of C(2000), thus for a connection at the middle of a beam, to find the compliance difference between the cracked and intact state as follows (see Fig.19).

The part above the crack (stiffness $I_2 = b(1-\alpha)^3 h^3 / 12$) carries a moment M_3 and normal force N and the part below the crack (stiffness $I_1 = b\alpha^3 h^3 / 12$) carries a moment M_1 , normal force N and a shear force V . and at the end of the crack a negative moment of about: $M_2 \approx -M_1$. Further is $M_2 = M_1 - V\lambda$, thus $M_1 = V\lambda / 2$.

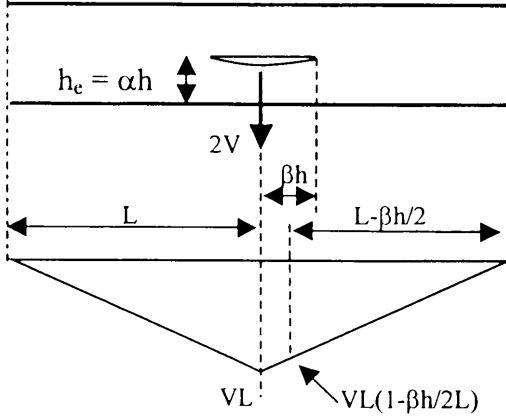


Fig. 19. Beam with crack by the dowel

The deformation of beam 2 of the cracked part βh is equal to the uncracked deformation δ_{un} of that part and the deformation of beam 1 is δ_{un} plus the crack opening δ (see Figure 19 and 20) and δ is

$$\begin{aligned} \delta &= \frac{1}{2} \cdot \frac{V\lambda^2}{EI_1} \cdot \frac{2}{3} \cdot \lambda - \frac{1}{2} \frac{M_1 \lambda^2}{EI_1} = \\ &= \frac{1}{3} \cdot \frac{V\lambda^3}{EI_1} - \frac{1}{4} \cdot \frac{V\lambda^3}{EI_1} = \\ &= \frac{1}{12} \cdot \frac{V\lambda^3}{EI_1} = \frac{V\beta^3}{bE\alpha^3} \end{aligned} \quad (11)$$

The deflection difference of the cracked and uncracked state, including shear, is total:

$$\delta = \frac{1.2}{G} \left(\frac{\beta h}{b\alpha h} - \frac{\beta h}{bh} \right) \cdot V + \frac{V\beta^3}{bE\alpha^3} \quad (12)$$

The condition of equilibrium at crack length β is:

$$\partial(V \cdot \delta / 2 - G_c b \beta h) / \partial \beta = 0 \text{ or: } \left\{ \partial(\delta / V) / \partial \beta \right\} \cdot V^2 / 2 = G_c b h$$

$$\text{or: } V_f = \sqrt{\frac{2G_c b h}{\frac{\partial(\delta / V)}{\partial \beta}}} \quad (13)$$

where G_c is the fracture energy. It follows from eq.(12) that:

$$\frac{\partial(\delta / V)}{\partial \beta} = \frac{1.2}{bG} \left(\frac{1}{\alpha} - 1 \right) + \frac{3\beta^2}{Eb\alpha^3} \quad (14)$$

and eq.(13) becomes:

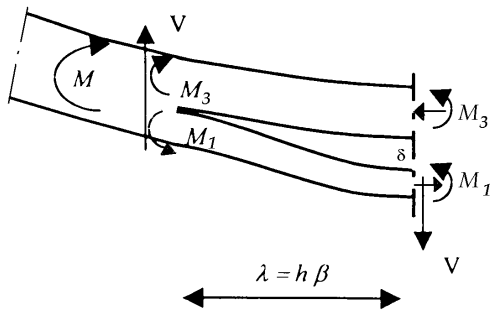


Fig. 20. Statics of half the crack.

$$V_f = b\alpha h \sqrt{\frac{GG_c / h}{0.6(1-\alpha)\alpha + 1.5\beta^2 G / (\alpha E)}} \quad (15)$$

giving, for the always relatively small values of β , the previous for end-notches found equation:

$$\frac{V_f}{b\alpha h} = \frac{\sqrt{GG_c / h}}{\sqrt{0.6 \cdot (1-\alpha) \cdot \alpha}} \quad (16)$$

(see C(1990)) which thus also applies for notched beams and for end-joints and verifies the lower bound of the strength, predicted by the theory.

This shows that only work by shear stress contributes to mode I fracture (elastic shear stress

dissipation). This linear elastic fracture mechanics derivation is not enough because design should be based on “flow “ of the joint (embedment flow) before splitting of the beam and the interaction of joint failure and beam splitting has to be regarded. Because plastic flow of the dowel also causes crack opening, splitting also occurs as secondary failure after hardening of the dowel strength. By the finite element empirics, this splitting is regarded as the ultimate strength state of the connection. This means that a huge hardening for one- and two dowel joints is accepted and hardly any hardening as final state for multi dowel connections and a difference in strength definition of every dowel is accepted. For the new definition of the strength of the connection, as splitting strength the derivation has to be adopted as follows:

When crack extension starts of a cantilever beam loaded by a constant load V , giving a deflection increase of δ at V due to this crack extension, then the applied external energy to the beam is $V \cdot \delta$. The energy balance equation then is:

$$V\delta = V\delta / 2 + E_c \quad (17)$$

where $V\delta / 2$ is the increase of the elastic energy and E_c the energy of crack extension.

$$\text{Thus: } E_c = V\delta / 2 \quad (18)$$

Thus the energy of crack extension is equal to the increase of elastic energy.

Eq.(18) also can be written with de incremental deflection $\delta = du$:

$$E_c = V^2 d(u/V)/2 = G_f b h d(\beta) \text{ or:}$$

$$V = \sqrt{\frac{2G_f b h}{\partial(u/V) / \partial\beta}} \quad (19)$$

where G_f is the fracture energy per unit crack surface and “ $bhd(\beta)$ ” the crack surface increase with “ b ” as width and “ h ” the height of the beam with a crack length $l = \beta h$.

When the load on the cantilever beam, mentioned above, is prevented to move, the energy balance, eq.(17) becomes:

$$0 = E_e + E_c, \text{ or: } E_c = -E_e = -V\delta / 2 \quad (20)$$

for the same crack length and now the energy of crack extension is equal to the decrease of elastic energy in the beam.

When the joint at load V becomes determining and just start to flow at δ_1 when splitting of the beam occurs, (design value of equal strength of joint and beam), then eq.(17) becomes:

$$V\delta = (V\delta_1) / 2 + V(\delta - \delta_1) + E_c \quad (21)$$

where again $V\delta_1 / 2$ is the increase of the elastic energy and $V(\delta - \delta_1)$ the plastic energy of the flow of the joint. From eq.(21) then follows:

$$E_c = V\delta_1 / 2 \quad (22)$$

the same as eq.(18)..

For dowel connections, plastic deformation in the last case will not yet occur because it is coupled with crack extension. When the dowels of the joint are pressed into the wood, the crack opening increases and thus also crack extension. It can be seen in eq.(21), that when flow occurs, the total applied external energy $V\delta$ is used for plastic deformation. This is a comparable situation as given by eq.(20), and the at the plastic flow coupled crack extension will cause a decrease of the elastic energy. Eq.(21) thus for joints is:

$$V\delta = (V\delta_1 - \delta_2) / 2 + V(\delta - \delta_1) + E_s \quad (23)$$

where $V\delta_2 / 2$ is the decrease of the elastic energy by the part of crack extension due to the plastic deformation. From eq.(23) now follows:

$$E_s = V(\delta_1 + \delta_2) / 2 \quad (24)$$

and eq.(19) becomes:

$$V = \sqrt{\frac{2G_f bh}{\partial((u_1 + u_2) / V) / \partial\beta}} \quad (25)$$

From eq.(22) and (24) follows that $V_c \delta_{1c} = V(\delta_1 + \delta_2)$, where $V_c \delta_{1c}$ is the amount when the connection is as strong as the beam (according to eq.(21). Thus:

$$\frac{\delta_1 + \delta_2}{\delta_{1c}} = \frac{V_c}{V} = \frac{n_c V_n}{n V_n} = \frac{n_c}{n} \quad (26)$$

where V_n is the ultimate load of the dowel at flow and n the number of dowels.

Substitution of eq.(26) into eq.(25) gives:

$$V = \sqrt{\frac{2G_f bh}{\partial(u_{1c} / V) / \partial\beta}} \cdot \frac{n}{n_c} \quad (27)$$

what is equal to $\sqrt{n/n_c}$ times the strength according to eq.(19) for $u = u_{1c}$, thus $\sqrt{n/n_c}$ times the splitting strength of the beam as is applied in C(2000),

According to eq.(23), the theoretical lower bound of V according to eq.(27) occurs at $\delta_1 = \delta_2$,

Thus when $n/n_c = 1/2$. In C(2000), the empirical value of 0.5 to 0.4 is mentioned according to the data giving:

$$V = \sqrt{\frac{2G_f bh}{\partial(u_{1c} / V) / \partial\beta}} \cdot \sqrt{0,45} = \sqrt{\frac{2G_f bh}{\partial(u_{1c} / V) / \partial\beta}} \cdot 0,67 \quad (28)$$

This requirement for “flow” of the joint at failure: $\sqrt{GG_f} = 0,67 \cdot 18 = 12 \text{ Nmm}^{-1.5}$ is included in the Eurocode (see § 7.1 of C(2000)).

The condition $\delta_1 = \delta_2$ means that there is sufficient elastic energy for total unloading and thus full crack extension with sufficient external work for plastic dissipation by the joints. According to eq.(23) is for that case:

$$E_c = V \delta_1 \quad (29)$$

Because, for real safety, thus for the by law demanded, calculable reliability, design has to be based on theory, and not on intrinsic not general empirical rules, (as e.g. of Ehlbeck at all (1989)), the precise, theoretical exact rules, derived in vd Put C(1990), were accepted in Building Regulations in 1990. For the first time then was shown, and accepted, that fracture mechanics has to be applied for exact design of joints loaded perpendicular to grain. Ten years later, the theoretical design equations were adapted for the allowed, prolonged plastic embedment flow of dowels, in C(2000), according to the new vision of CIB-W18, that splitting failure of joints should be prevented by separate design rules. The theoretical, and thus precisely fit rules above remain necessary for strength calculation. However to prevent splitting is, as Eurocode 5 design rule, explicitly prescribed that dowel failure, has to be below the, theoretical and empirical confirmed, lowest possible splitting strength.

Just see also C(2014b), to notice that, in contrast with Fig. 16, the given numerical data (of LVL) fit to the theory with a COV of 10 %. Also even the rigorously simplified design equations of vdPut C(1990) are precise enough for all given data at that time. In C(2000) the derived theoretical lowest splitting force of 0.67 times the maximal value is verified by all joint types of Ehlbeck et al (1989). Clearly the COV of 10% confirms empirically the exact approach because this can not be improved by any other method.

In C(2000), the full derivation of the $\sqrt{n/n_c}$ -factor of the Compliance method was not

given. By error all appendices with theory were left out. The article was delivered as Atari-file what is not compatible with Word and the article was retyped by the co-author, what caused many errors. Also a new data-fit was done, leading then to a worse fit. The reason is probably that the co-author uses the theory equations in his further publications as if they are empirical equations (which should not fit precisely to the data) to compare these with the always solely empirical equations of other publications. This comparison of arbitrary fitting is the only possible level of communication due to the censorship of exact theory discussion in CIB-W18. Due to this censorship criticism on exact theory is freely possible, even any nonsense is publishable, but defense on such comment is prohibited, because defense would contain a proof based on exact theory what is prohibited and thus censored. As example of such comments of the in this Section discussed theory, (see C(2000)) for joints loaded perpendicular to grain, for which it was decided by Larsen and members of the Eurocode 5 Committee and agreed by the CIB-W18 conference, to prescribe, in Eurocode 5, always determining dowel failure below the lowest splitting boundary, where below there is not enough energy for total splitting, the following: This simple, by everyone chosen, lower splitting boundary, is by nearly everybody regarded to be the mean splitting strength to make a cheap rejection possible. The mean strength equation which fits precisely to all known data of these type of joints is eq.(1a) or Eq.(27):

$$V_f = b\alpha h \sqrt{\frac{GG_c / h}{0.6(1-\alpha)\alpha + 1.5\beta^2 G / (\alpha E)}} \cdot \sqrt{\frac{n}{n_c}} \quad (1a)$$

The lower boundary occurs theoretically when $n \leq 0.5n_c$, but according to the data of Ehlbeck (1989) is this lower boundary about: $n \approx 0.45n_c$. Thus the lowest value of:

$$\sqrt{n/n_c} \geq \sqrt{0.45} = 0.67.$$

Eq.(1a) contains the influence of initial crack length of $2\beta h$. The influence of the initial crack length is extensively discussed in vdPut C(1990). The dowel deformation determines the initial crack-length increase. It appears that the term with β is small in eq.(1a) and even negligible, leading to:

$$\frac{V_f}{b\alpha h} = \frac{\sqrt{GG_c / h}}{\sqrt{0.6 \cdot (1-\alpha) \cdot \alpha}} \cdot \sqrt{\frac{n}{n_c}} \quad (2a)$$

There is no significant better fit of eq.(1a) with respect to eq.(2a). Eq.(2a) can be regarded as the highest lower bound of V_f and thus the closest to the real solution, which thus applies for the lowest possible initial crack lengths. The maximal value of eq.(2a) for under-designed ($n \geq n_c$) dowel strength capacity, eq.(3a):

$$\frac{V_f}{b\alpha h} = \frac{\sqrt{GG_c / h}}{\sqrt{0.6 \cdot (1-\alpha) \cdot \alpha}} \quad (3a)$$

is the reason why Jensen suggest the theory to be not right because it only is based on shear strength with a zero initial crack length. (The fact that elastic shear stress dissipation determines mode I fracture has nothing to do with failure of the beam by shear loading).

Based on the data of Ehlbeck et al (1989) is the mean value of $\sqrt{GG_c} = 18 \text{ N/mm}^{1.5}$ and the lowest splitting force, when $\sqrt{n/n_c} = 0.67$, is: $\sqrt{GG_c} = 0.67 \cdot 18 = 12$, Thus:

$\sqrt{GG_c / 0.6} = 15.5 \text{ N/mm}^{1.5}$. The characteristic value, to be chosen by the Code committee should be in the order of $15.5 \cdot 2/3 \approx 10 \text{ N/mm}^{1.5}$, giving:

$$V_f \leq 10b\sqrt{h_e / (1-h_e / h)} \quad (4a)$$

The dowels should be dimensioned in such way that embedment flow occurs at this value of the splitting strength (according to CIB-W18 and the Code committee).

Eq.(4a) is now a grateful equation to reject theory, by wrongly comparison with the empirical mean strength in CIB-W18 papers. Therefore everyone

1) left out the factor $\sqrt{n/n_c}$ when regarding mean strength. Only Leijten (2001) had no negative conclusion, indicating the right use of eq.(4a) as lowest value for splitting.

2) Ballerini (2004): did not remember the rule he voted for, and stated (by looking only at eq.(4a)), that the design formula neglects any influence of the connection geometry, although this is estimated by exact theory, given by eq.(1a), and, he clearly did not remember, that not splitting, but always initial dowel failure, is determining and thus that the dowel geometry is perfectly present and accounted.

3) By Franke en Quenville (2010) the same error is made. Their given empirical numerical data and later data (e.g. LVL of Fig. 16) are analyzed in C(2014b) showing that the theoretical formula (2a) fits to their data precisely with a COV of 10 %. Thus clearly is demonstrated that the initial crack length β term is not needed in eq.(1a) for precise design.

4) Jensen (2012) CIB-W18/45-7-2, Also does not know that initial failure is by the dowels showing a perfect dowel geometry. He mentioned the zero initial crack length, showing he did not notice eq.(1a), but, his (2003) publication shows that he, as only one, noticed that the strength equation (3a) exists, by stating that it is based on shear stress only with zero initial crack length. However he does not know that this elastic shear stress dissipation for mode I failure, has nothing to do with shear failure of the beam. A better conclusion would have been that clearly the critical distortional energy principle (derived in A(2009)) always applies. Thus design of joints should be according to the lower bound equilibrium method regarding equilibrium of all involving parts and can not be given in design rules only.

C.3. References:

- Boström (1992), Method for determination of the softening behavior of wood etc. Thesis, Report TVBM-1012, Lund, Sweden.
- Wu E.M (1967) Application of fracture mechanics to anisotropic plates. J Appl Mech 34:967–974.
- Mall S., Murphy J.F., Shottafer J.E. (1983), “Criterion for Mixed Mode Fracture in Wood” J. Eng. Mech. 109(3) 680-690, June 1983.
- A(1982a) A general failure criterion for wood, Proc. IUFRO Timber Engineering Group Meeting, Boras, May 1982.
- A(2009) A continuum failure criterion applicable to wood, J Wood Sci 55:315–322.
- B(2011) A new theory of nucleation, in: Phase Transitions: A Multinational Journal, 84:11-12, 999-1014.
- C(1990) Tension perpendicular to the grain at notches and joints, CIB-W18A/23-10-1.
- C(2000) Evaluation of perpendicular to grain failure of beams caused by concentrated loads of joints CIB-W18/33-7-7
- C(2007a) Softening behavior and correction of the fracture energy Theor Appl Frac Mech 48 (2007) 127–139
- C(2007b) A new fracture mechanics theory of orthotropic materials like wood, Eng Frac Mech 74 (2007) 771-781
- C(2011a) A new fracture mechanics theory of wood”, Nova Science Publishers, New York,.
- C(2011b) Fracture mechanics of wood and wood like reinforced polymers Nova Science Publishers, Inc.

- C(2012) Discussion of: “Mode II fracture mechanics properties of wood measured by the asymmetric four-point bending test using a single-edge-notched specimen of H Yoshihara in Eng. Frac. Mech. 75 pp 4727-4739” in Eng. Frac. Mech. 90 pp 172-179 .
- C(2013) Comment on: ”Mode II critical stress intensity factor of wood measured by the asymmetric four-point bending test of single-edge-notched specimen while considering an additional crack length, of H. Yoshihara in Holzforschung, Vol. 66, p 989-992, 2012”. This comment was censored by Yoshihara as “editor” and could not be published.
- C(2014) Exact derivation of the geometric correction factor of the center notched test specimen, based on small cracks merging as explanation of softening; Under review
- D(2008b) Derivation of the bearing strength perpendicular to the grain of locally loaded timber blocks Holz Roh Werkst, 66 p 409-417.

References of the questionable comments

- Ehlbeck J, Görlacher R, Werner H. (1989) Determination of perpendicular to grain tensile stresses in joints with dowel-type fasteners, CIB-W18, paper 22-7-2, G.
- Ballerini, M. (2004) CIB-W18/37-7-5.
- Franke, B. Quenneville P. (2013) CIB-W18/46-7-6.
- Franke, B. and Quenneville, P. (2010), CIB-W18/43-7-6 + World Timber Conf. Trentino
- Leijten, A.J.M. (2001) CIB-W18/35-7-7.
- Jensen, J.L., Quenneville, P., Girhammar, U.A. and Kallsner, B. (2012), CIB-W18/45-7-2.
- Jensen, J.L. (2003) CIB-W18/36-7-8/9.

Additional theory extensions by vdPut.

- Explanation of the mixed mode interaction equation and energy principle of wood.
In: P. Morlier, G. Valentin; Cost 508; Workshop on Fracture mechanics in wooden materials. April, 9-10 1992. Bordeaux, 1993, p. 85-92.
- Modified energy approach for fracture of notched beams.
In: P. Morlier, G. Valentin, (eds.); Workshop on Fracture mechanics in wooden materials. Cost 508; April, 9-10 1992. Bordeaux, 1993, p. 93-100.
- Energy approach for fracture of joints loaded perpendicular to the grain.
In: P. Morlier, G. Valentin, (eds.); Workshop on Fracture mechanics in wooded materials. April, 9-10 1992. Cost 508. Bordeaux, 1993, p. 101-109.
- Discussion of the failure criterion for combined bending and compression.
Meeting 24 of CIB-W18, Oxford UK, September 1991. Oxford, 1992, p. 13-23.
- The SED (Strain Energy Density) criterion of Sih is extended for orthotropic wood in the Appendix of C(2007a) and approved by Sih as Editor of the Theor. Appl. Frac. Mech. J.